Predicting Subjective Discomfort Associated with Lens Distortion in VR Headsets During Vestibulo-Ocular Response to VR Scenes

Tsz Tai Chan, Yixuan Wang, Richard Hau Yue So and Jerry Jia

Abstract— With advances in Virtual Reality (VR) technology, user expectation for a near-perfect experience is also increasing. The push for a wider field-of-view can increase the challenges of correcting lens distortion. Past studies on imperfect VR experiences have focused on motion sickness provoked by vection-inducing VR stimuli and discomfort due to mismatches in accommodation and binocular convergence. Disorientation and discomfort due to unintended optical flow induced by lens distortion, referred to as dynamic distortion (DD), has, to date, received little attention. This study examines and models the effects of DD during head rotations with various fixed gazes stabilized by vestibulo-ocular reflex (VOR). Increases in DD levels comparable to lens parameters from poorly designed commercial VR lenses significantly increase discomfort scores of viewers in relation to disorientation, dizziness, and eye strain. Cross-validated results indicate that the model is able to predict significant differences in subjective scores resulting from different commercial VR lenses and these predictions correlated with empirical data. The present work provides new insights to understand symptoms of discomfort in VR during user interactions with static world-locked / space-stabilized scenes and contributes to the design of discomfort-free VR headset lenses.

Index Terms— Virtual reality, lens distortion, visual discomfort, motion sickness, disorientation, vestibulo-ocular reflex

1 Introduction

COMMERCIAL VR headsets currently rely on optics to project pixels on a head-steered near-eye display in order to form images of space-stabilized virtual worlds [1]. To create a realistic virtual world, the geometry and texture of a 3D object needs to be accurately reproduced spatially. The spatial mapping between the display and virtual world is critically important to geometric reproduction. With advances in VR technology, users expect a perfect mapping experience when involved in world-locked VR scenes in which all virtual objects remain spatially stable relative to the physical world (i.e., world-stable). As a result, images of a VR world-locked object will be visible, and appear spatially stable, when their angular positions fall within the field-of-view of a head-steered VR display. In practice, the mapping is not perfect because the transmitted light field from a VR display is different from the naturally occurring light field from a real environment that the virtual world-locked VR scenes are simulating [1] (Fig. 1a). The issue is attributed to the optical layout of VR headsets. The optical layout of a VR headset can be considered as an ideal lens with extra lens distortions.

Theoretically, a distortion correction process to pre-transform a displayed image should be able to cancel out any distortion by the lens. This can be achieved with ray tracing and calibration through a set of mapping files generated specifically to all locations on the display. Fig. 1a illustrates how a distorted display can be corrected; Fig. 1b presents a 2D spatial transformation in the form of a 2D map.

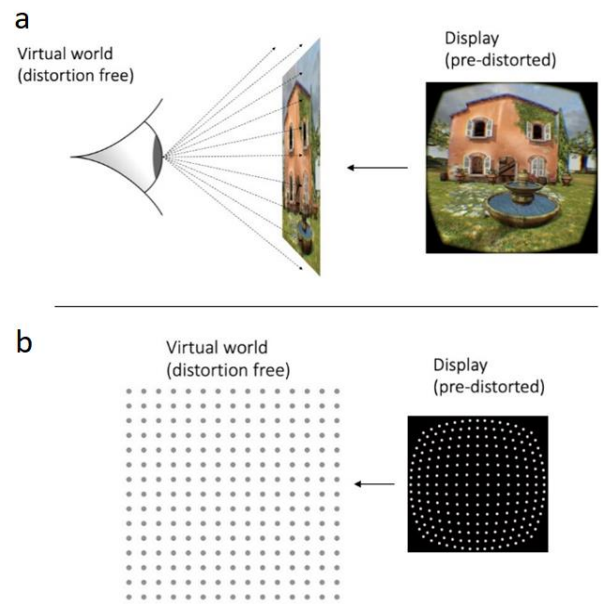

Fig. 1. (a) Distortion correction in a VR headset allows virtual content to appear regular and normal. (b) Example of a distortion correction map that is independent of content and saved on the VR headset.

- *T.T. Chan is with the Department of Industrial Engineering and Decision Analytics, The Hong Kong University of Science and Technology, Hong Kong, China. E-mail: ttchanac@connect.ust.hk.*
- *Y. Wang is with the Department of Chemical and Biological Engineering, The Hong Kong University of Science and Technology, Hong Kong, China. E-mail: ywanggx@connect.ust.hk.*
- *R. H. Y. So is with the Department of Industrial Engineering and Decision Analytics and Department of Chemical and Biological Engineering, The Hong Kong University of Science and Technology, Hong Kong, China. E-mail: rhyso@ust.hk.*
- *J. Jia is with the Facebook Reality Laboratory, CA, USA. E-mail: Jerry.Jia@fb.com.*

(T.T. Chan and Y. Wang are co-first authors.)

xxxx-xxxx/0x/$xx.00 © 200x IEEE Published by the IEEE Computer Society

This article has been accepted for publication in a future issue of this journal, but has not been fully edited. Content may change prior to final publication. Citation information: DOI 10.1109/TVCG.2022.3168190, IEEE Transactions on Visualization and Computer Graphics

During the calculation of the correction mapping files, a fixed pupil location relative to the lens is assumed; however, this assumption does not hold in many situations. One typical example where this assumption fails is during reading with the help of vestibule-ocular reflex (VOR), a response to stabilize the eye gaze during head movements. When a viewer turns his / her head while keeping the eye gaze stable (VOR-type movement), the eye pupil will move relative to the lens in the opposite direction of the head movement to continue to fixate on the object of attention (see Fig. 2). Thus, the assumption of a fixed pupil location relative to the lens is violated, and a dynamically changing distortion (referred to as "dynamic distortion (DD)") results from the incomplete correction.

The DD can cause observations of "shifting floors" and "curved walls". As floors and walls are fixtures that are normally not moving, their movements may affect the reference rest frame's judgment and even lead to motion sickness symptoms, such as disorientation and dizziness according to the rest frame hypothesis [2, 3, 4]. A review of relevant literature failed to find any study of DD among VR users. In this study, we refer to symptoms of motion sickness induced by the DD during VOR-type head motions as "DD-VOR discomfort". The occurrence of DD-VOR discomfort, if proven, can be an example to support the rest frame hypothesis (RFH) of motion sickness [2, 3, 4]. From the perspective of sensory conflict theory [5, 6], the mismatch between visual and vestibular inputs could also be an explanation for DD-VOR discomfort.

The occurrence of motion sickness symptoms among VR users has stymied the growth of the industry. Most previous studies on VR discomfort focused on hardware or vection-provoking visual content. Regarding hardware, the effect of display latency has been the subject of many studies [7, 8, 9, 10, 11]. As to the influence of visual content on motion sickness, the effects of vection-provoking visual stimuli has also been the subject of many studies [12, 13, 14, 15, 16]. Solutions to reduce discomfort have been proposed [12, 13, 17, 18]. Examples include reduction of field-of-view [17, 18, 19] and controlling the speed of navigation [12, 13]. Models have also been proposed to predict vection induced motion sickness [20, 21].

In summary, despite advances in VR technology, discomfort and motion sickness symptoms are still prevalent among users. While effects of hardware (e.g., display latency) and vection induced VR content have been the focus of research, motion sickness due to imperfect lens correction (DD-VOR discomfort) has received little attention. One possible reason for the lack of a study on DD-VOR discomfort among VR users is that it takes a collaborative effort between the VR headset manufacturer and the researchers to manipulate and control the relevant parameters. This paper reports the first study to examine the DD-VOR discomfort and proposes a predictive model. In this study, we focus on the effects of DD-VOR discomfort caused by lens distortion. Both the influence of the vection-provoking scenes and latency are controlled. All VR scenes remain world-locked static without passive navigation. Users can still choose what they see through head steering. The latency is around 10ms or less with displays updated at 90Hz.

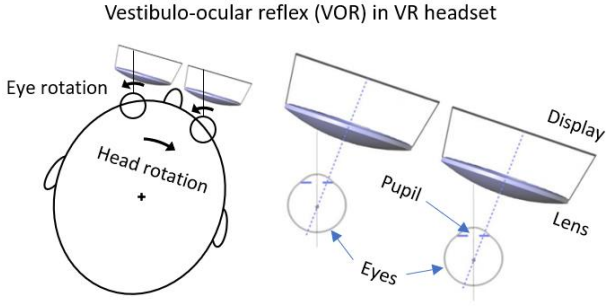

Fig. 2. Vestibulo-ocular reflex in VR headset leads to angular displacement of pupils related to the near-eye display. Before VOR movement, the pupil is looking through the center of the lens; and after the VOR movement, it is looking at the same displayed object but through the side of the lens.

2 Causes Of DD-VOR Discomfort

The historical development of the theoretical understanding of DD-VOR discomfort can be summarized as three progressive steps: (i) sensory conflict theory, i.e., the theory that humans suffer motion sickness due to conflict in received sensory cues; (ii) physical causes; and (iii) sensory conflict theory specifically applied to DD-VOR. These three steps are broadly similar to the three levels of DD-VOR discomfort users experience.

2.1 Sensory conflict theory

Motion sickness is a general syndrome characterized by symptoms such as nausea, stomach discomfort, cold sweats and disorientation [2, 6]. About one-third of the population is currently susceptible to this condition with a range from moderate to extreme nausea [22]. A widely accepted hypothesis for motion sickness is sensory conflict theory [6, 23], which is also referred to as sensory rearrangement theory [5]. It proposes that the conflict among motion information perceived from different sensory modalities (e.g., vestibular, visual, and proprioceptive systems) and the expected sensory inputs based on previous experience can provoke discomfort [5, 6]. The sensory conflict theory has received support from reported correlations among perception of sensory conflict, neural activation at the reticular formation in the brainstem, neural activation of the autonomic nervous system and reported symptoms of motion sickness [24].

Studies of motion sickness among users of virtual reality systems have led to the development of the rest-frame hypothesis (RFH) [25]. This hypothesis predicts that the brain adopts the intrinsic Euclidean frame of reference to process spatial information. The rest-frame refers to some specific spatial features which an observer assumes to be space stationary (i.e., world-locked) [2, 4]. If DDs cause an assumed space stationary feature in a virtual environment to move, it would induce sensory mismatch and, hence, motion sickness [25].

2.2 Physical cause of DD

The pupil location is a vital factor in causing DD. Pupil locations relative to a VR lens will shift if the eyes rotate relative to the head. If, initially, the eye's gaze is aligned

This article has been accepted for publication in a future issue of this journal, but has not been fully edited. Content may change prior to final publication. Citation information: DOI 10.1109/TVCG.2022.3168190, IEEE Transactions on Visualization and Computer Graphics

with the optical axis of the VR lens, during a VOR-type head movement when the gaze is fixated ahead, the lens rotates away with the head forcing the pupil location to move off the optical axis of the lens as illustrated in Fig. 3.

With the dynamic change of pupil location, light from the same pixel on the display is received at slightly different angular directions into the eye. More importantly, it is passing through a different part of the lens and subjected to different lens distortion. If pupil locations are known, current technology can predict and correct the lens distortion through a ray-tracing program [26]. Fig. 4 illustrates an example of such a correction procedure. The lens distortion is illustrated by arrays of red dots on a black angular grid. At 0 degrees (before VOR), there is no lens distortion. When the head has turned 20 degrees (after the VOR), red dots shift from the intersection points indicating the corresponding optical distortion which is angular position dependent and lens dependent. If we connect each pair of corresponding red dots after the VOR with its black interaction point, we can create a 2D vector field across the field-of-view of the lens (Fig. 5). This 2D vector field is also called optical flow. Fig. 5 illustrates the optical flow from three different existing commercial VR lens designs simulated with VOR head movements from 0 to 20° to the right direction of the user.

2.3 DD-VOR Discomfort explained by sensory conflict theory

DD occurs when a VR user is performing a VOR-type head movement (Fig. 5). In this scenario, as the head motion is initiated and driven by the user, the inertial sense of motion (i.e., the vestibular cue) is perfectly perceived. Due to DD, the visual input is distorted, causing a sensory conflict and its subsequent discomfort and motion sickness. One example is research conducted by Stratton (1897) who examined the effects of wearing inverted and reversed lens. Even though the vestibular input was perfectly perceived, the locomotion and general psychomotor performance were disturbed due to distorted visual inputs. The

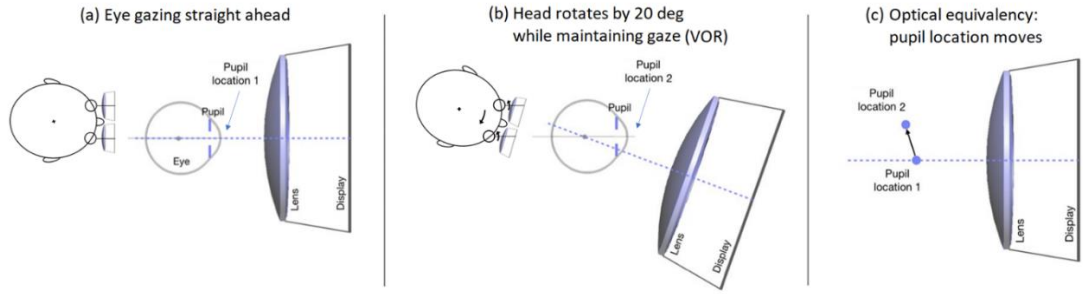

Fig. 3. (View from top of the head) Optical root cause for DD: during VOR, eye pupil location changes relative to the lens. This changes the perceived distortion pattern of the lens accordingly.

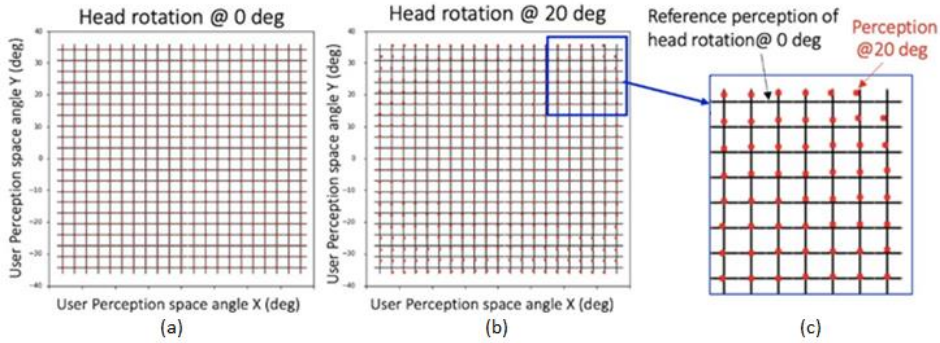

Fig. 4. Illustrations of lens distortion by angular grids (grid size is approximately 3.3 by 3.3 degrees). (a) The grid is not distorted when the head is pointing straight ahead. (b, c) After a 20° rightward head rotation, the grid is distorted as illustrated by the red dots representing the interaction points after distortion.

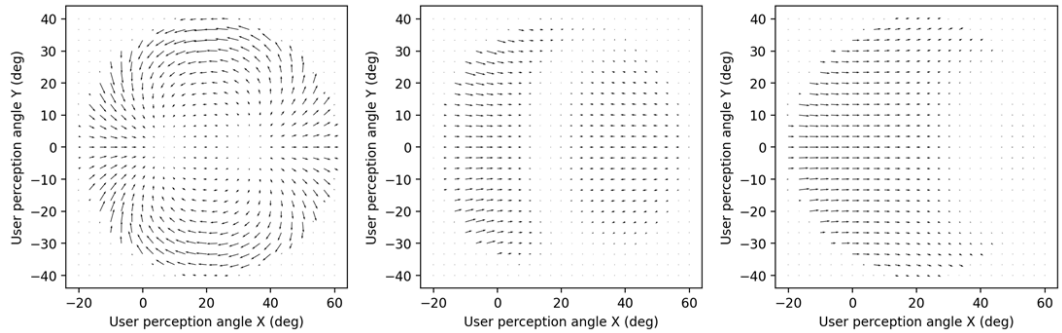

Fig. 5. 2D vector field (i.e., optical flow) representations of the DD induced by a rightward 20° head rotation with three different lenses. Each vector is a line connecting the black intersections and red dot in Fig. 4. Both axes are in degrees and vectors have been magnified 10 times for better illustrations.

This article has been accepted for publication in a future issue of this journal, but has not been fully edited. Content may change prior to final publication. Citation information: DOI 10.1109/TVCG.2022.3168190, IEEE Transactions on Visualization and Computer Graphics

participant reported discomfort and nausea on the first and second day. On removing the lens after an adaptation period, the participant also experienced symptoms of nausea [27]. Likewise, participants experiencing DD-VOR are hypothesized to report discomfort. DD-VOR discomfort can be accounted for by the sensory conflict theory, and specifically, it could be a supportive example for the RFH. In the real world, the information about self-motion, object motion, and rest-frame can be inferred from visual cues without disturbance, and that information will be consistent with those inferred by inertial cues from the vestibular systems. However, in VR and augmented reality (AR), when an observer makes VOR-type head movements, due to the afore-mentioned DD, the visual cues presented to the observer will be incorrect. The observable effect is "visual distortion" where visual cues are unexpected and occasionally annoying. Examples of reported observations in these cases include: "the edge of building is distorted", "straight frames look bent", etc. In addition, observers may infer self-motion and / or orientation that are inconsistent with those inferred from the inertial cues. Prolonged exposure to such conflict can lead to symptoms of motion sickness in susceptible populations. Fig. 6 illustrates the logic of how sensory conflicts can be induced by visual distortion through a block diagram with a comparison between the visual-vestibular interactions in the real world and the VR world.

3 Model Development

3.1 Verification of motivation of model development: significant DD-VOR discomfort effects

Before developing the model, a user study was conducted to verify the strength of the effects. Two dynamic distortion conditions were derived from a lens (lens A): one with a scaling factor of 0.5 (A-1), the other with a scaling factor of 2 (A-2). The scaling factor was defined to magnify (scaling factor > 1) or reduce (scaling factor < 1) the dynamic distortion. It was hypothesized that condition A-2 would be associated with significantly higher discomfort ratings. Participants (n=8, see Section 4.3) were exposed to each of the two selected conditions for a total of 20 minutes. During this time, they were asked to focus on a central eye-fixation point and turn their heads 16° to 20° to the right and back and repeated according to a 100-bpm metronome (see more details in Section 4). At the end of the test, they rated the DD-VOR discomfort they experienced, with a number from 0 to 5. Before and after the 20-minute test, they were also asked to fill in Simulator Sickness Questionnaires (pre-SSQ and post-SSQ) [28]. Results indicated that the SSQ scores were significantly increased after the 20-minute exposure for both DD conditions (paired t-tests, mean pre-SSQ and post-SSQ scores of A-1 condition: 0.935 vs. 20.10, $p = 0.0008$; mean pre-SSQ and post-SSQ scores of A-2 condition: 1.40 vs. 23.38, $p=0.0019$). Also, the A-2 condition resulted in significantly higher DD-VOR discomfort scores than A-1 condition at the end of the 20-minute test (paired t-test, $p = 0.0098$, Fig. 7). Examinations of the symptoms reported in the SSQ questionnaires indicate that "general discomfort," "vertigo," and "fullness of head" were more frequently reported in A-2 than in A-1 condition (increases from 37.5% to 62.5% to 75%). Results of the verification study confirms the presence of a genuine and significant DD-VOR discomfort effect.

3.2 Overview of the model development process

Based on the above verified significant effects of visual distortion and symptoms of motion sickness, an analytical model was developed and trained with data collected in further studies (see Section 4). The model starts with the selection of lens design and the pupil location relative to the center of the lens. As illustrated in Figs. 3, 4 and 5, optical flow in terms of 2D vector field representing the DD was generated (Section 3.3). The optic flow was then

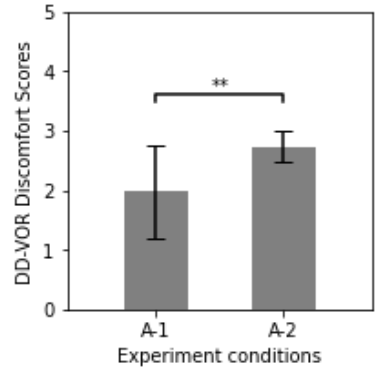

Fig. 7. Significant higher DD-VOR discomfort scores were reported for the dynamic distortion conditions with aggravated distortion.

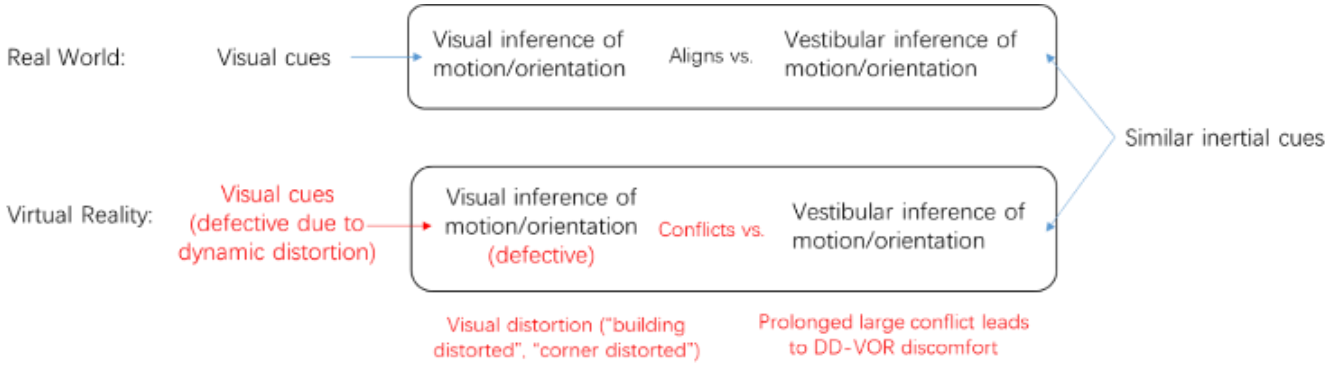

Fig. 6. Framework for understanding discomfort during VOR-type head motion. In the real world, consistent sense of motion can be inferred from visual cues and inertial cues (top) not in VR or AR (bottom). Defective visual cues produce conflicts

This article has been accepted for publication in a future issue of this journal, but has not been fully edited. Content may change prior to final publication. Citation information: DOI 10.1109/TVCG.2022.3168190, IEEE Transactions on Visualization and Computer Graphics

passed through a series of mathematical operations to account for (i) eccentricity effects (Section 3.4); (ii) spatial-temporal interactions (Section 3.5); and (iii) influence in terms of 16 optic flow pattern features (Section 3.5).–The processed DD features were mapped to predicted DD-VOR discomfort scores and distortion scores through a regression model (Section 3.6). The regression model was pre-trained using data from the psychophysical experiment (see Section 4). Fig. 8 illustrates the procedure of how the model predicts DD-VOR discomfort and distortion scores associated with the use of a particular lens in VR applications.

3.3 Quantification of dynamic lens distortions using optical flow

The DD can be represented by an optical flow map (a 2D vector field) with a fixed radius of 40 degrees from lens center and step size of 3.3 degrees (Fig. 9). As illustrated in Figs. 3, 4 and 5, an optical flow map is generated between the pupil location when the VOR starts, and the pupil location when the VOR ends using optical ray tracing. This is referred to as the uncompensated optical flow (Fig. 9a). The displayed content at the fixation point will shift according to the optical flow (i.e., distortion). To maintain the fixation, the eyes will move to follow the displayed content through smooth pursuit, and the perceived optical flow would be different from the uncompensated optical flow map. To account for the effects of corrective eye movements, the optical flow map is recalibrated by subtracting the vector at the new fixation point from the original, resulting in compensated optical flow (Fig. 9b). In this study, the compensated optical flow was used. Fig. 10 illustrates the optical flow representing the DD, after corrective eye movements, of the four lenses studied in the experiment. The DDs were associated with a rightward head rotation of 20 degrees. Kindly note that Fig. 10 is just a snapshot; in the study, DD was dynamically updated according to the measured head rotations.

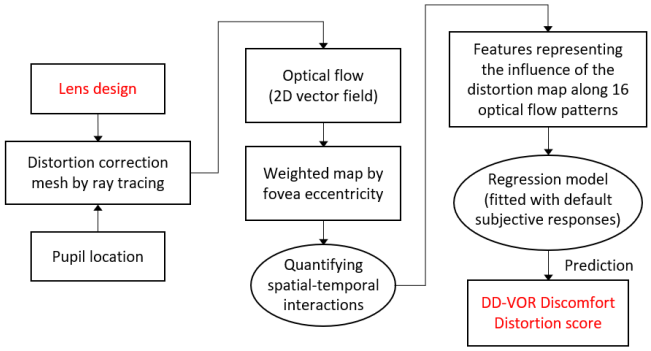

Fig. 8. Block diagram illustrating how the model predicts DD-VOR discomfort and distortion scores to be expected from users of VR headsets fitted with a particular lens.

3.4 Sensitivity weighting of distortions according to eccentricity

Past studies reported that visual sensitivity decreases with eccentricity, and that the rate of changes of sensitivity along the horizontal axis and the vertical axis are different [29, 30, 31]. Literature on the motion sensitivity during VOR-type head motion is absent. As a first attempt, we followed the past literature and applied the reported visual sensitivity weighting (see Fig. 11). In summary, visual distortion closer to the eye fixation point (i.e., foveal) has a higher influence on users. We acknowledge that this weighting is only preliminary and can be changed in the future.

3.5 Quantifying spatial-temporal interactions between VOR head movements and distortions

Two elements were used to quantify the optical flow representations of DDs for scoring its influence on subjective responses; one relates to distortion intensity, the other relates to distortion pattern. For distortion intensity, the magnitudes of all vectors (v_i) in an optical flow such as one of those illustrated in Fig. 10 were averaged as a scalar

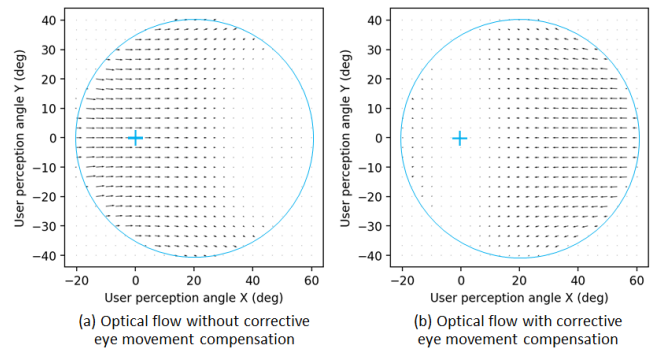

Fig. 9. (a) Example of uncompensated optical flow without considering the corrective eye movement. X, y axes are virtual angle space with reference to fixation as a blue cross. (b) Compensated optical flow based on center plot where the whole map is subtracted by the vector at the fixation point (blue cross).

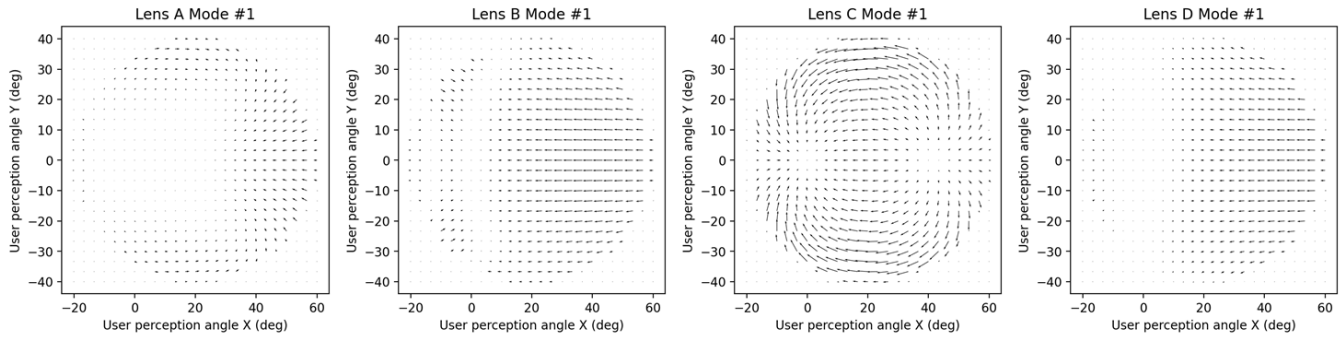

Fig. 10. Optic flows representing the DD after corrective eye movements for the four lenses studied in the experiment. The DD was specific to a rightward head rotation of 20 degrees. Both axes are in degrees and the vector magnitude have been scaled up 10 times for ease ~~of~~ of visualization.

This article has been accepted for publication in a future issue of this journal, but has not been fully edited. Content may change prior to final publication. Citation information: DOI 10.1109/TVCG.2022.3168190, IEEE Transactions on Visualization and Computer Graphics

(S) (in degrees). A natural log function was then applied to estimate the perceived strength of stimuli (M) with reference to the Weber-Fechner's law. As the threshold stimulus S_0 is unknown, a manually tuned value of 0.016 degrees was used for modeling purposes based upon the minimum dynamic distortion threshold collected in pilot runs. A value of "1" was added before the logarithmic operation to enable continuing prediction of M for S more, equal, or less than S_0. The relevant equations are as follows:

$$M = \ln\left(\frac{S}{S_0} + 1\right), \qquad where\ S = \frac{1}{n}\sum_{i}^{n}\|v_i\| \tag{1}$$

In Eqt. (1): S, S_o, vi are same as explained in the text, and n is the total number of vectors in each optical flow.

As explained in Section 2.3, DD-VOR discomfort can be caused by conflicting perceived motion (Fig. 6). We propose to decompose distortion patterns into components along translational and rotational axes from an egocentric viewpoint. As a first attempt, the total distortion represented by optical flow is decomposed into 16 components according to 16 patterns: upward, downward, rightward, leftward, expansion, contraction, clockwise (CW), anti-clockwise (anti-CW), expansion-X, contraction-X, shear-X-CW, shear-X-anti-CW, expansion-Y, contraction-Y, shear-Y-CW, and shear-Y-anti-CW (Fig. 12). The selection of component directions is mainly based on optical flow associated with natural motions such as going forward (expansion), plus a few patterns such as shear, to relate to the distortion score. Each of the 16 components is determined by applying dot product between the vectors in the original optic flow and the corresponding component pattern. Then, the component distortion intensity S_i is calculated as the average vector's magnitude from the resulting optic flow after the dot product operation. In summary, the original lens distortion as represented by the optic flow is decomposed into 16 feature components. The decomposition of a lens distortion into 16 features will enable finer mapping between distortions and subjecting discomfort (Section 3.6).

A weighting parameter p_i is then defined for each component as a measure of the alignment of vectors of a particular pattern with the vectors of the original optic flow representing the lens distortion:

$$M_i = p_i \ln\left(\frac{S_i}{S_0} + 1\right) \tag{2}$$

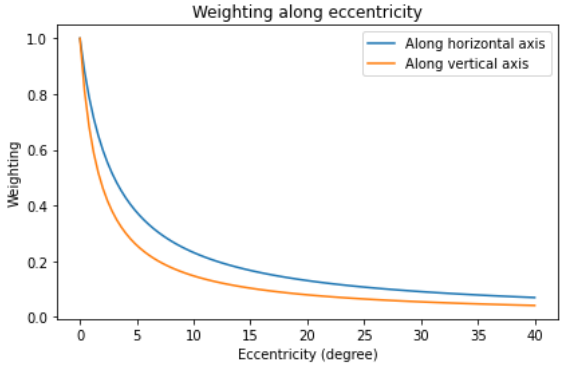

Fig. 11. Visual sensitivity weightings along the horizontal and vertical axes along the eccentricity of the location of in the FOV based on [29, 30 and 31].

where i is the index for the distortion pattern component and has a value from 1 to 16 for indexing the 16 patterns. The process of calculate p_i is illustrated in Fig. 13. The higher the alignment, the larger the value of p_i. This has been achieved by calculating the angle difference between the corresponding vectors in the original optic flow and a particular pattern flow. This generates a distribution of angles, and, by fitting a von Mises distribution, the probability of angles within -15 degrees and 15 degrees is extracted to be the parameter p_i which has a value from 0 to 1. The values of p_i were determined by the DD pattern. Different lens designs and pupil deviations from the center of the lens would lead to different p_i values. In other words, for the same head rotations (hence pupil deviations), different lenses will have different weighting distributions of p_i values. Likewise, for the same lens, different head rotations will result in different weighting distributions of p_i values.

3.6 Modeling subjective ratings as functions of the featured distortion

Following the above steps, the optical flow representing the lens distortion can be transformed to a 16-dimensional feature vector array (M). This "M" quantifies the perceived dynamic distortion during a VOR (DD-VOR). Values of M are completely objective and can be calculated for any lens and any VOR movement with known starting and end locations. To establish the correlational relationships between this objective arrays M and the subjective visual discomfort scores, a regression model is used to estimate the DD-VOR discomfort and distortion scores as follows:

$$Score = a(M^T\beta + \varepsilon) \tag{3}$$

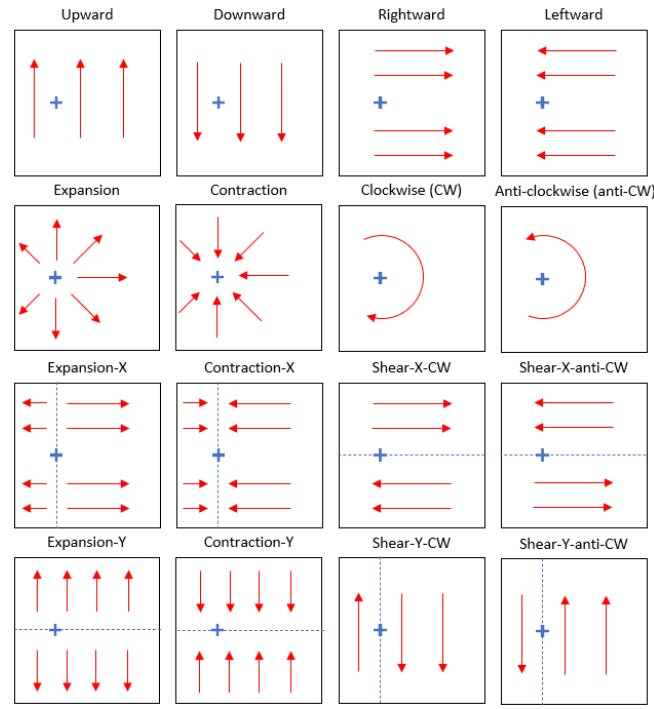

Fig. 12. 16 different patterns with reference to fixation at the blue cross The red arrows represent the expected distortion direction of the pattern. These patterns will be used as masking filter to extract and decompose a lens distortion into 16 components.

This article has been accepted for publication in a future issue of this journal, but has not been fully edited. Content may change prior to final publication. Citation information: DOI 10.1109/TVCG.2022.3168190, IEEE Transactions on Visualization and Computer Graphics

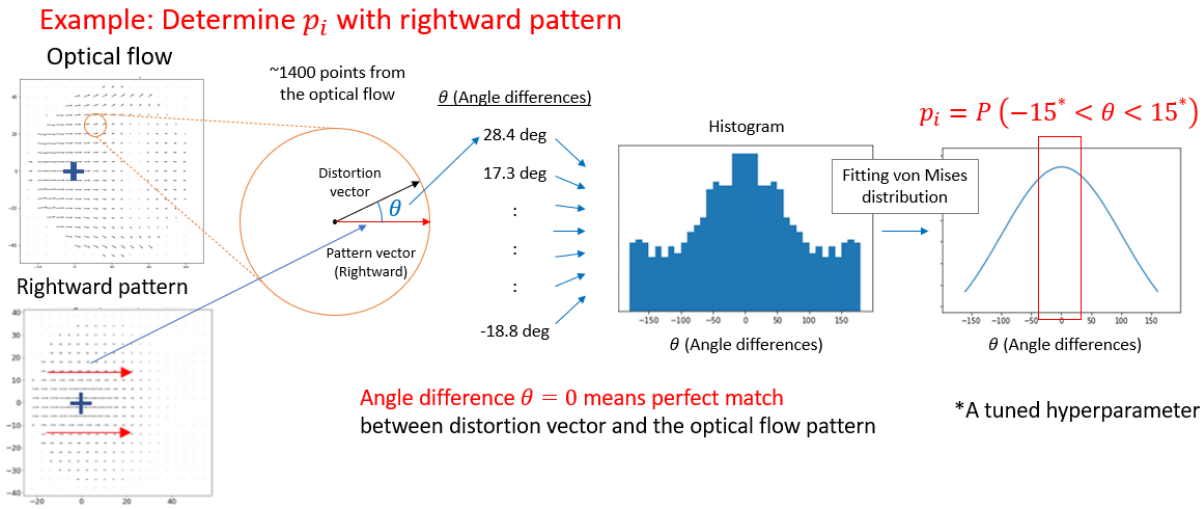

Fig. 13. Illustration of procedure, using the rightward component as example, to calculate each component's probability values of p_i : how likely the viewer will observe this corresponding component.

where "Score" is either the measured DD-VOR discomfort score or the distortion score (see Section 4 on psychophysical experiments); "a" represents a constant accounting for inter-subject variability in motion sickness and distortion susceptibility; "β" is the parameter array relating the subjective severity scores to M (the 16 vector maps) featuring the qualified DD-VOR; and "ε" represents other factors contributing to the score that was not controlled or not in scope of study. The values of a, β and ε were estimated through regression models to fit the reported data in the valuation experiments to be described in the following sections with minimizing mean-squared error. In particular, "α" was estimated from the data to represent the data variances due to individual variations, hence, individual susceptibility while "β" was estimated from the data to represent mean (of subjects) data variances due to M (the 16 vector maps), hence, average influence of M.

4 Psychophysical Experiments

4.1 Objectives and hypothesis

To explore the perceptual effects of the dynamic distortion, we conducted two experiments. We intended to verify, by manipulating the visual distortion perceived by participants during the experiment, that the dynamic distortion would induce subjective discomfort and other motion sickness symptoms like disorientation and dizziness (DD-VOR discomfort). It was hypothesized that the visual distortion would be correlated with the DD-VOR discomfort. We hypothesized that conditions with larger dynamic distortion magnitudes would lead to more severe reported DD-VOR discomfort (H1), and lenses with different distortion would cause noticeable differences in subjective scores (H2).

4.2 Variables and designs of experiment

4.2.1 Independent variables: DD conditions

Four lenses (A, B, C and D) were used in the experiment. They were provided by the partnering company and the model names have been hidden. To expand the diversity of dynamic distortion conditions to be investigated, we simulated five modes (mode #1, #2, #3, #4 and #5) of distortion patterns based on the existing lens designs and four levels of absolute average intensity (average vector magnitudes: 0.05, 0.10, 0.15, 0.20 degrees) (see Table 1). These provided 80 different conditions (4 lenses x 5 modes of patterns x 4 levels of intensity). In addition, the original lens distortions were scaled to 0.5, 1 and 2 times of their intensity. These are the 12 conditions (4 lenses x mode 1 – the intrinsic pattern x 3 scaling factors). The original intrinsic distortion patterns were represented by the condition with mode 1 and unity scaling factor. The definitions of modes are documented in Table 1. Modes 1

TABLE 1
DYNAMIC DISTORTION CONDITIONS TESTED IN THE FIRST EXPERIMENT

Lens	Mode (Variants of lens)		Intensity of Distortion
A B C D	#1	Original lens distortion	For all 5 modes, four levels of average intensity (S = 0.05, 0.10, 0.15, 0.20 degrees) were adopted (80 conditions). For 4 lenses in mode #1, 3 scaling factors (0.5x, 1x, 2x) were adopted (extra 12 conditions).
	#2	Lens distortion from 0 to 10° was applied during head rotation from 0 to 10°.	
	#3	Lens distortion from 10 to 20° was applied during head rotation from 0 to 10°.	
	#4	Lens distortion from 20 to 30° was applied during head rotation from 0 to 10°.	
	#5	Lens distortion from 0 to 32° was compressed and applied during head rotation from 0 to 16 degrees.	

This article has been accepted for publication in a future issue of this journal, but has not been fully edited. Content may change prior to final publication. Citation information: DOI 10.1109/TVCG.2022.3168190, IEEE Transactions on Visualization and Computer Graphics

to 4 used regional distortion patterns extracted from the 4 lenses and mode 5 used spatially compressed distortion patterns extracted from the 4 lenses. These modes were designed to expand the range of lens distortion to be studied. In this paper, data associated with the original intrinsic lens distortions are reported.

4.2.2 Dependent variables: Subjective distortion and discomfort

To obtain a quantitative perceptual evaluation of conditions of dynamic distortion, we used two predictive subjective scales (Figs. 14 and 15). If we allow participants to stay in each of the 92 VR conditions for 20 minutes to incubate measurable symptoms, the experiment will take at least 2 years to complete as participants will need more than 7 days to recover between conditions to reduce the effects of learning [32]. To study this phenomenon in an efficient way, we first examined all the 92 conditions in a single study with short exposures (1-2 minutes). To verify the accuracy of the predictive scores, a second validation experiment with two representative conditions selected from the 92 conditions was conducted. During this validation experiment, 20-minute exposures were used for each condition (Table 1, Section 4.6). The two conditions were generated from the original distortion of lens A with scaling factors of 0.5x and 2x.

In the first experiment, all participants were exposed to each of the 92 DD conditions for a short duration (about 1-2 minutes) in random order. After each exposure, they were asked to predict, with a number from 0 to 5, the possible severity of dizziness, disorientation, and discomfort if they were in that condition for 20 minutes (Fig. 14). The number is referred to as "DD-VOR discomfort score" in the following text. Similarly, their perceived difference in deformation/ distortion were rated on a separate scale, the Distortion Scale (Fig. 15). For this question, participants were asked to give a number from 0 to 3, which is referred to as a "distortion score".

4.3 Participants

A pilot test with three participants was conducted to estimate the optimal sample size to distinguish two dynamic distortion conditions. They were asked to report the DD-VOR discomfort scores for a series of conditions including two target conditions: lens C-mode #1 and lens D -mode #1. Assuming that the two averaged DD-VOR scores (2.633 for lens C-mode #1 and 1.367 for lens D-mode #1) and the standard deviation of the difference was 0.833, a power analyses for the paired sample t test was conducted. Results indicated that at least six participants were needed to get a desired power of 0.80 at the significance level of 0.05 for the main effects that we were seeking [33].

Nine participants (four females) from the Hong Kong University of Science and Technology with normal or corrected-to-normal vision participated in the experiment. One male participant discontinued his participation due to discomfort, and his data was therefore not included in the subsequent analyses. Informed consent was obtained from all participants, and the experiment was approved by the Human Research Ethics Committee of the Hong Kong University of Science and Technology. None of the eight participants took part in the pilot test.

4.4 Method and procedures

4.4.1 Method

A modified commercial headset based on Oculus Rift CV1 with a customized lens module and software provided by Facebook was used. Its intrinsic DD is close to the median of the four lenses. The display resolution was 1440 × 1600 per eye (roughly 21 pixels per degree), the refresh rate was 90 Hz and the FOV was about 100 degrees. A visual scene full of buildings was created based on Unity (Unity 2018.3.0 release) with a virtual asset called "*Windridge City*" accessible through the Unity asset store (Fig. 16). A white sphere in the middle of FOV with a diameter of 0.025°, was the fixation point. The distance from the observer and the fixation point was eight meters.

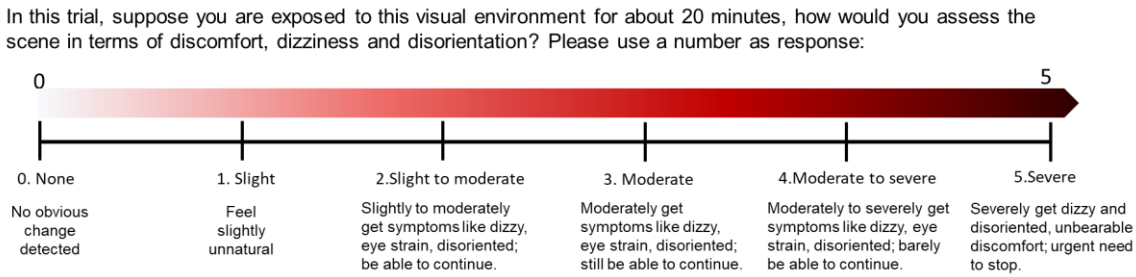

Fig. 14. Dizziness, disorientation, and discomfort scales used in the experiment. Both the English and Chinese translations were shown to the participants.

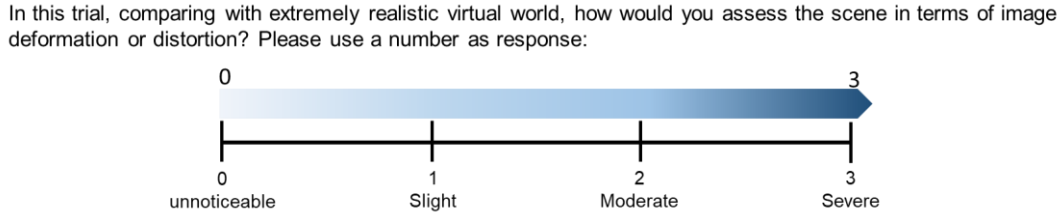

Fig. 15. Distortion scale used in the experiment. Both the English and Chinese translations were shown to the participants.

This article has been accepted for publication in a future issue of this journal, but has not been fully edited. Content may change prior to final publication. Citation information: DOI 10.1109/TVCG.2022.3168190, IEEE Transactions on Visualization and Computer Graphics

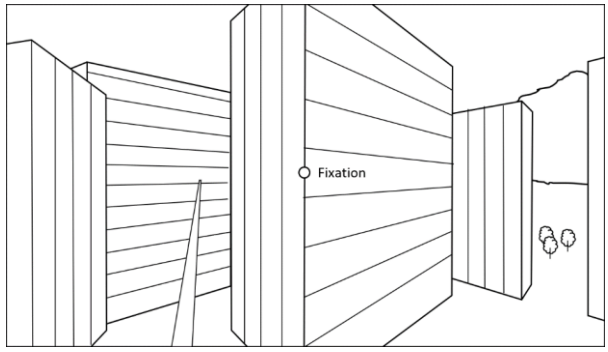

Fig. 16. Simplified illustration of a subject's view in the experiment. The virtual environment used was more sophisticated, but the license agreement does not allow public display or reproduction of it.

The head motion of each participant was trained to be similar in the range from 16° to 20° to the right with a 100-bpm metronome. Head motion was controlled with a visual feedback training session; a metronome was used as the audio cue to regulate the head motion frequency. When the rotation angle reached 16°, a short visual feedback bar on the fixation point switched from horizontal to vertical. When the rotation angle went over 20°, the vertical bar would turn back and remain horizontal. Hearing the metronome beats, participants would finish a round-trip head rotation between 0 and the range of 16° to 20° in two beats, and then rest for another beat. Fig. 17b illustrates the visual feedback bar, and Fig. 17b shows examples of typical head motion time histories of the participants. This visual feedback bar was used throughout the training but was removed during the actual experiment to avoid distraction to the participants. Measured head motions indicated that participants were able to maintain their head movements within the 16° to 20° range (Fig. 17b).

4.4.2 Procedure

Participants were required to keep focusing on the fixation point and rotate their heads back and forth from center to the right (in a range from 16 to 20 degrees). The background visual stimulation was space stationary (i.e., world-locked), and the only visual motion was from the dynamic distortion when participants were carrying out a VOR-type head motion. Participants were thoroughly briefed on the procedure and the questions that they were going to be asked. In the training sessions, ten to fifteen conditions were randomly selected to enable participants to become familiar with the procedure with the use of the visual feedback bar as a control of head motion magnitude. With several head rotations, they were able to report scores for the presented condition. In the main experiment, the visual feedback bar was removed as the participants were well trained in controlling their head motions already. Measured head motions indicated that the participants were able to maintain their head motions within the range of 16 to 20 degrees (Fig. 17B). Both the DD-VOR Discomfort scores and distortion scores were collected for each condition following the same procedure. The presentation order of conditions was randomized, and there was a break for five minutes after twelve conditions to avoid fatigue.

4.5 Results and analyses

When we compared the original distortion conditions (mode #1, scaling factor 1x) of the four lenses, different perception scores were reported (Fig. 18). Data have been tested to be normally distributed (Shapiro-Wilk test, DD-VOR discomfort score: $p = 0.49$; distortion score: $p = 0.22$). Results of paired t-tests showed significant differences in reported distortion scores and predicted DD-VOR discomfort scores between lenses A and C (DD-VOR discomfort score: $p = 0.0157$; distortion score: $p = 0.0057$), between lenses A and D (DD-VOR discomfort score: $p = 0.0038$; distortion score: $p = 0.0056$), between B and C (DD-VOR discomfort score: $p = 0.0067$; distortion score: $p = 0.0015$), between lenses B and D (DD-VOR discomfort score: $p = 0.031$), and between lenses C and D (DD-VOR discomfort score: $p = 0.0041$; distortion score: $p = 0.0014$). The distortion score and DD-VOR discomfort score were strongly correlated (Pearson's $\varrho = 0.746$, $p<0.001$).

The average DD-VOR discomfort scores by the lens, mode and intensity are illustrated in Fig. 19. The potential of the lenses to provoke DD-VOR discomfort is in the order of C>B≈A>D. DD-VOR discomfort scores for different modes were found to be roughly the same. The means of DD-VOR discomfort scores increased with the intensity. This supports hypotheses H1 and H2 and demonstrates the importance of correcting lens distortion in future VR headsets.

Results of the analyses of variance (ANOVAs) on DD-VOR discomfort scores of 80 conditions (excluding the 12

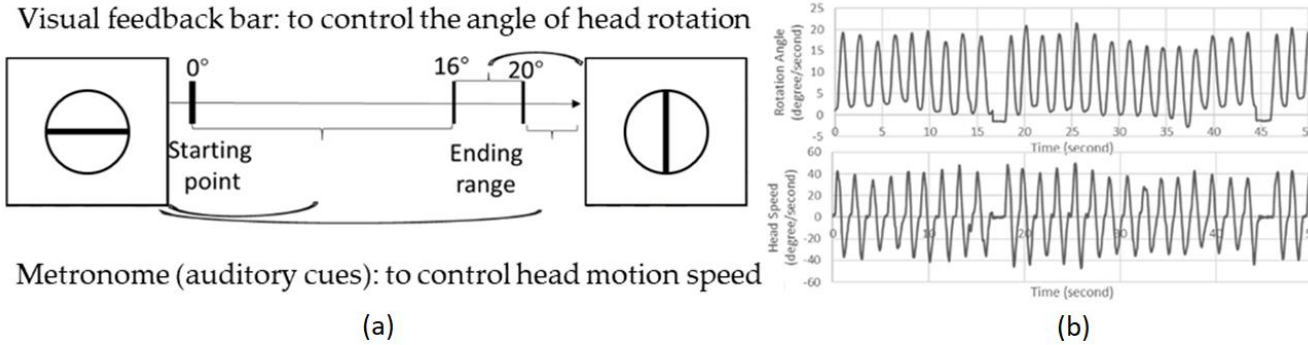

Fig. 17. Illustrations of how head motion was controlled in the experiments. Participants were trained to rotate head horizontally to the right to a range of 16 to 20° and back to 0°. (a) During the training session, participants could see a black bar through the fixation point and hear a 100-bpm metronome. The bar turned vertical when the head rotated in the range of 16 to 20° and horizontal when the head rotation was out of that range. (b) Recorded head movement time histories indicate that during the experiment, the head motion roughly ranged from 16 to 20° oscillating in a uniform frequency.

This article has been accepted for publication in a future issue of this journal, but has not been fully edited. Content may change prior to final publication. Citation information: DOI 10.1109/TVCG.2022.3168190, IEEE Transactions on Visualization and Computer Graphics

intrinsic lens distortion conditions) rated by all participants showed that the main effects of type of lens, mode, average intensity of distortion and the interaction between lens and average intensity were found to be significant [Lens: $F(3, 21)=12.440$, $p<0.001$; Mode: $F(4, 28)=3.114$, $p=0.031$, Average intensity: $F(3, 21)=32.969$, $p<0.001$; Lens*Average Intensity: $F(9, 63)=6.130$, $p<0.001$]. Post hoc analysis indicated that, except between lens A and B, the differences between reported discomfort scores associated with each pair of lenses were significant. The differences between different intensity levels were also statistically significant.

4.6 Second experiment: to validate the accuracy of participants' prediction of discomfort

The validity of the predicted score was verified using scores collected from the same participants after 20-minute exposures to selected conditions. Two conditions of lens A with original distortion (mode # 1) were selected: one with a scaling factor of 0.5 (A-1) and the other with a scaling factor of 2 (A-2). The same group of participants was exposed to each of two selected conditions for 20 minutes with gazes focused on a fixation point and the same horizontal head motion. At the end of each exposure, the same group participants were asked to rate the DD-VOR discomfort they experienced with a number from 0 to 5. Before and after each 20-minute exposure, they were asked to fill in the Simulator Sickness Questionnaire (SSQ) adopted from [28] to record their symptoms and corresponding severity. Each exposure was separated by at least 7 days. To verify if the predicted DD-VOR discomfort score used in the experiment was indicative of the actual discomfort reported after a 20-minute exposure, we compared two sets of scores. The scores predicted within a short period were significantly correlated with the scores rated after the 20-minute test (Pearson's $\rho = 0.521$, $p = 0.038$). Results of test-and-retest comparisons indicated that the predicted and actual DD-VOR discomfort scores are statistically consistent (Cronbach's $\alpha = 0.773$)[34]. The result verified that the quick predictive rating questions as shown in Fig. 14 were able to measure the predictive discomfort, dizziness, and disorientation scores as if after the 20-minute exposure.

5 Model Results And Applications

Subjectively reported data from the experiment were used to estimate parameters in the model through an optimizer by minimizing mean-squared error between the ratings and predicted score. To evaluate the model results, the data from the experiment was separated into a training set and a testing set. One of the goals of this study was to estimate the performance of the design of a new lens, which is the lens B in the experiment. The testing set was therefore made up of subjective reported data of lens B conditions. The rest of the data from lenses A, C and D formed the training set.

5.1 Training and Results

Fig. 20 illustrates the results of a comparison between reported scores and predicted scores in the experiment categorized into a training set and a testing set. The

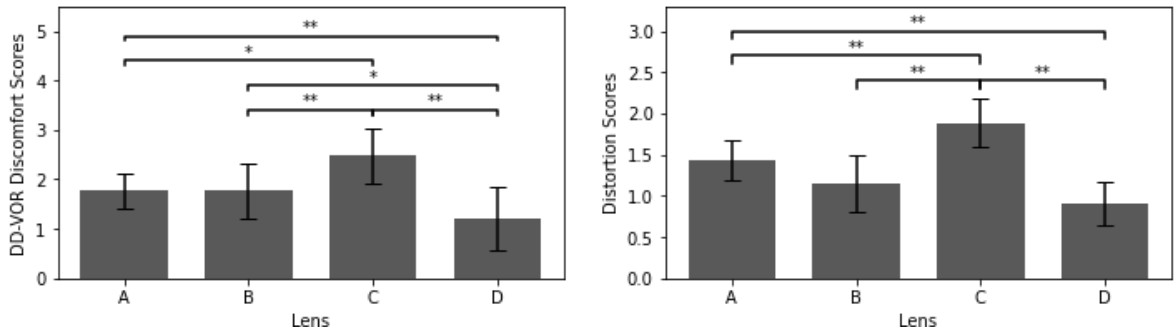

Fig. 18. Comparison of DD-VOR discomfort scores (Left) and distortion scores (Right) for the four original lens conditions (lens A, B C and D, mode #1). The significant differences in corresponding perception scores between lenses are labelled with asterisk(s) in each figure (Paired t-test, * for $p < 0.05$ and ** for $p < 0.01$).

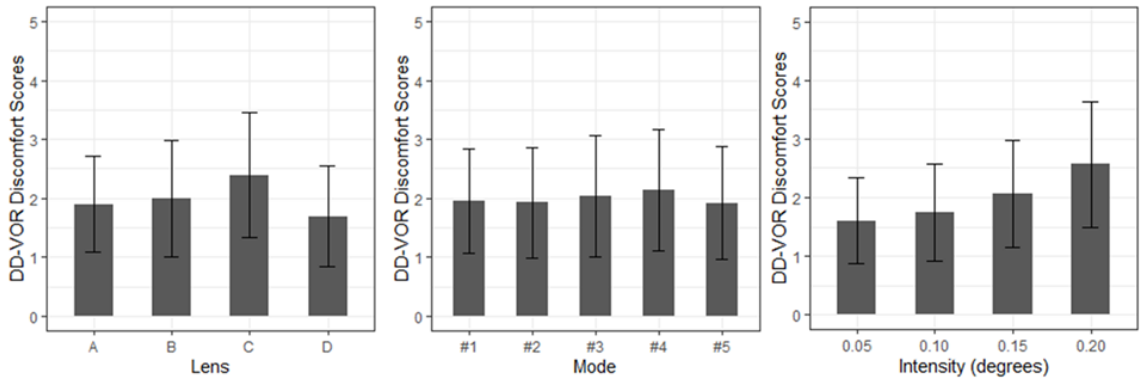

Fig. 19. Mean DD-VOR discomfort scores of different lenses, modes, and average intensity: data from 80 conditions (4 lenses * 5 modes * 4 Average intensities). Results of ANOVA can be found in the text. Main effects of lens and average intensity are significant ($p<0.001$).

This article has been accepted for publication in a future issue of this journal, but has not been fully edited. Content may change prior to final publication. Citation information: DOI 10.1109/TVCG.2022.3168190, IEEE Transactions on Visualization and Computer Graphics

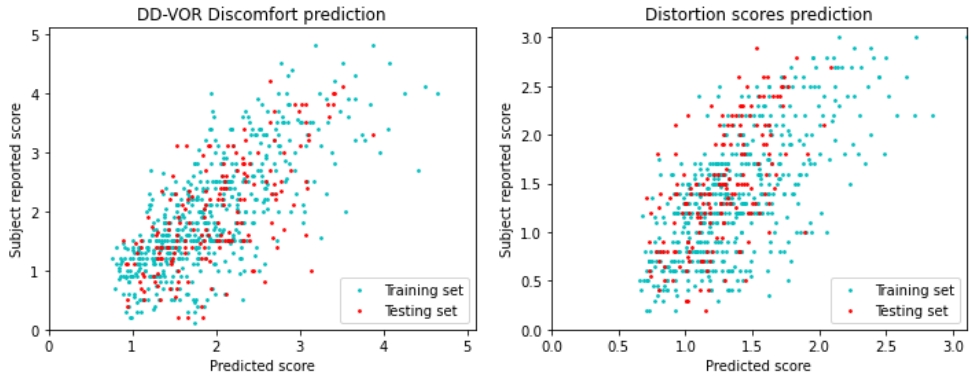

Fig. 20. Comparison of reported scores and predicted scores. Each dot represents a tested condition from a participant in the experiment.

prediction generally aligned with the data from the experiment. To benchmark the model, a naïve baseline model using mean value of ratings as the prediction was compared. Five-fold cross-validation was conducted by randomly splitting the training dataset into 5 equal sized groups, where each validation using 4 groups' data as training data and 1 group's data as the validation test data. Results are summarized in Table 2, where mean absolute error (MAE), root-mean-square error (RMSE), normalized RMSE (NRMSE) by dividing range of measured data, and R-squared values are shown. Comparing the NRMSE, the model performed slightly better in predicting DD-VOR discomfort than Distortion scores, as shown in Table 2, which may be because the design of the 16 features in the model leaned towards global optic flow of self-motion. A skewed outcome in Distortion score prediction is also observed in that the model tends to over-estimate the low-severity conditions and under-estimate the high-severity conditions.

5.2 Predicting new lens performance

To evaluate the model's ability to predict the lens's overall performance, data are grouped by different lens designs, and the comparison between mean predicted scores and reported scores are plotted as bar charts in Fig. 21. The prediction outcomes of DD-VOR discomfort by lens were comparable to the mean reported scores, including the test lens (i.e., lens B used in the experiment), while the Distortion score prediction was under-estimated for the test lens (Fig. 21). This suggests there may be some optical features that were not captured by the current version of the model. Further investigations of the DD patterns of the four lenses indicated that DD of lens B has more neighboring optic flow vectors that are abruptly different while the corresponding changes are smoother with the other three lenses (Fig. 10). Future work is needed. We also acknowledge that the current 16 patterns as shown in Fig. 12 covers more than just the horizontal axis which was the dominating axis of head rotations investigated in the experiments. Indeed, internal weightings (p_i) inside the model also confirm this observation. Future research will involve head rotations in all directions.

TABLE 2
MODEL PERFORMANCE METRICS

	DD-VOR discomfort scores				Distortion scores			
	MAE	RMSE	NRMSE	R-squared	MAE	RMSE	NRMSE	R-squared
Baseline model	0.764	0.942	0.200	0	0.502	0.622	0.222	0
Our model:								
Training set	0.501	0.642	0.137	0.536	0.371	0.457	0.163	0.461
5-fold cross-validation	0.513	0.653	0.140	0.503	0.382	0.470	0.168	0.427
Testing set	0.547	0.683	0.145	0.450	0.415	0.519	0.185	0.274

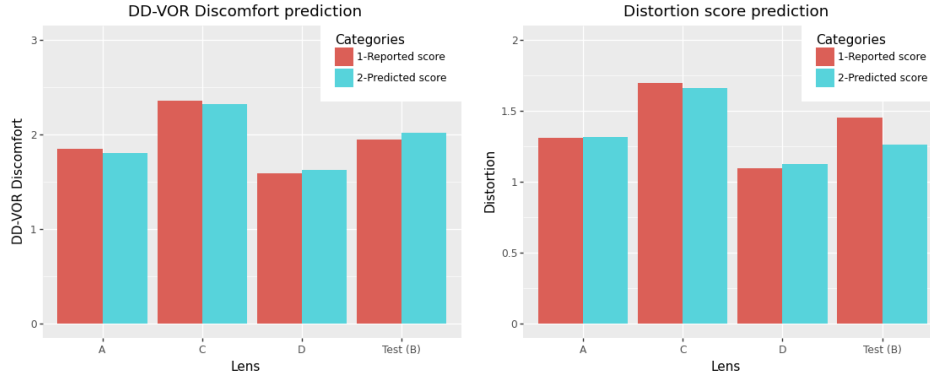

Fig. 21. Comparison of mean reported scores and predicted scores grouped by lens, including the test lens (lens B).

This article has been accepted for publication in a future issue of this journal, but has not been fully edited. Content may change prior to final publication. Citation information: DOI 10.1109/TVCG.2022.3168190, IEEE Transactions on Visualization and Computer Graphics

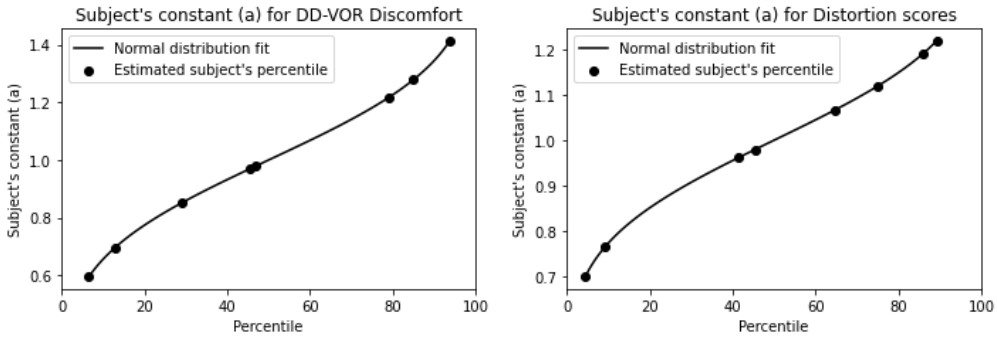

Fig. 22. Subject's constant (a) resulted from the model and corresponding percentiles estimated by normal distribution.

5.3 Estimating ratings at different percentiles of population

Subject's constants were used in the model development (3). To account for inter-subject variability, a normal distribution was fitted to the subjective predictive rating data of all subjects in the first experiment. A scale at different percentile of population can be estimated through the fitted curve as shown in Fig. 22 to determine an estimated specification for larger population in evaluating optical flow. When evaluating lens designs or optical flow's impact on human perception, the scale at the 90th percentile can be chosen to cover a larger population in scoring. In other words, the model can be used to predict the scores for a chosen percentile of population and can be used for the industry.

6 Discussion

With the public's increasing expectation of perfection in VR experiences, the quest for providing a discomfort-free VR experience is intensifying. Following the sensory conflict theory and the rest-frame hypothesis, motion sickness provoked with dynamic moving VR scene has been the subject of many studies [2 to 24]. The general conclusion is that a vection-inducing VR moving scene is a major cause of motion sickness. On the other hand, there are situations in which viewers experience discomfort during normal viewing of VR world-locked scenes without vection- inducing VR moving scenes. This latter situation is important, but research is incomplete. This study fills this gap by presenting empirical data as well as a validated prediction model. Results from the user experiments indicated that subjective discomfort (dizziness, disorientation) is significantly affected by the type of lens and intensity of visual distortion, with their two-way interactions being significant as well [Lens: $F(3, 21)=12.440$, $p<0.001$; Intensity: $F(3, 21)=32.969$, $p<0.001$; Lens*Intensity: $F(9, 63)=6.130$, $p<0.001$]. This is a new and important finding as it suggests that a VR user inspecting a world-locked VR scene could experience discomfort even in the absence of vection-inducing motion. For the first time, the dynamic distortion (DD) caused by lens during VOR type head motion has been shown to cause significant increases in discomfort, disorientation, and dizziness. Furthermore, a validated model to quantify and predict the subjective discomfort as functions of lens design has been reported.

6.1 Applications

The most direct application of the work is twofold. First, it provides concrete evidence that lens distortion remaining after correction by image pre-transformation, can cause visual discomfort, disorientation, and dizziness. Second, the model provides a tool to predict subjective discomfort associated with different lens designs. The scope of application of the current predictive models goes beyond just lens distortion during VOR. For example, camera distortion to image pixels in mixed reality VR design can also be represented in the form of optical flow and hence, the similar methodology reported in this study can be extended to predict the associated visual discomfort scores as well.

With the quest for VR headsets with a wider field-of-view, lens design and associated distortion correction methods become ever more challenging. The model presented in this study represents a way to digitally prototype and predict user feedback before manufacturing a lens. This will not only reduce costs but also enable greater experimentation on lens design.

The reported work represents the first study that has directly examined and modelled the influence of the remaining lens distortion in VR systems after their (imperfect) compensation that has erratically assumed the pupil locations always remain at the center of the VR displays. This remaining lens distortion is called dynamic distortion (DD). This work is new and is linked to the literature on visually induced motion sickness. As this DD occurs in nearly all VR systems, the authors hope that this first attempt will be followed by more research so that future VR users can enjoy discomfort-free experience.

6.2 Limitations and future work

Being the first attempt on this topic, we acknowledge that the present study has limitations. All DDs examined were associated with four commercial VR lens and rightward head rotations of 16 to 20 degrees. Also, only one virtual environment was tested with eight participants. Future work to examine more distortion conditions, different types of head motions and involve more participants are desirable. Due to non-disclosure agreement, we are unable to disclose the specific model numbers of the commercial lenses. Notwithstanding that, the representative distortion patterns of the 4 lenses used have been presented in Figs. 5 and 10.

The current prediction model underestimated the distortion scores for the test lens. One possible reason is the abruptly changing DD pattern leading to a jerky rather than smooth distortion. We acknowledge that none of the current 16 pattern features were designed to capture the abruptness of DD. More studies are needed to improve the prediction models.

We acknowledge that a perfect eye tracker can theoretically eliminate DD-VOR Discomfort by monitoring the pupil location and perform adaptive DD compensation. However, the shortest response delay of current state-of-the-art eye-trackers in VR is around 15 ms [35]. A saccade can have a speed up to 500 degrees per second and a delay of 15 ms will introduce non-trivial tracking error that can be counterproductive. Notwithstanding that, how the response delays of eye tracking system will affect DD-VOR discomfort and is there a minimal delay for eye tracking above which the use of eye tracking will be counter-productive will be desirable future work.

7 Conclusion

The current study investigated and modeled the perceptual effects associated with remaining uncompensated lens distortion. Such distortions can cause unintended optical flow, called dynamic distortion (DD), during head rotations. Experimental data indicated that increases in DD can significantly increase discomfort scores (called DD-VOR discomfort) and perceived image distortion ($p<0.001$, ANOVAs). A better design of lenses has been shown to significantly reduce DD-VOR discomfort ($p<0.001$, paired t-test). A model has been developed to predict DD-VOR discomfort and distortion scores for new lens designs. The predictions from the model are consistent with the results from the user experiments. The predicted ranking of lenses in terms of comfort is also found to be consistent with the expected quality of the lens design.

In summary, this study evaluated and predicted the user experience during a VR experience with headsets featuring different lens designs for the first time. The model developed in this study can guide the development of new designs of optical layout as well as–to evaluate performances of existing lenses. Since DD occurs in all VR lens, future work to improve and expand the scope of applications for the model is desirable.

Acknowledgements

This study is partially funded by Facebook Reality Laboratory and Hong Kong University Grants Council. The authors would like to thank Phil Guan and Brant Lewis from Facebook Reality Laboratory for their constructive comments, and Yudong He and Tingyi Wang for their help on conducting experiment.

Corresponding author: T.T. Chan

References

[1] G. A. Koulieris, K. Akşit, M. Stengel, R. K. Mantiuk, K. Mania, and C. Richardt, "Near-Eye Display and Tracking Technologies for Virtual and Augmented Reality," Comput. Graph. Forum, vol. 38, no. 2, pp. 493–519, May 2019.

[2] J. D. Prothero, "The Role of Rest Frames in Vection, Presence and Motion," 1998.

[3] D. Parker and J. Prothero, "A Unified Approach to Presence and Motionsickness," in Virtual and Adaptive Environments, CRC Press, 2003, pp. 47–66.

[4] Z. Cao, "The effect of rest frames on simulator Discomfort reduction," no. July 2017, 2017.

[5] J. T. Reason, "Motionsickness: a special case of sensory rearrangement.," Adv. Sci., vol. 26, no. 130, pp. 386–93, Jun. 1970.

[6] C. M. Oman, "Sensory conflict in motionsickness: an Observer Theory approach," in Pictorial Communication In Real And Virtual Environments, 1991.

[7] A. Kinsella, "The effect of 0.2 Hz and 1.0 Hz frequency and 100 ms and 20-100 ms amplitude of latency on simulatory sickness in a head mounted display," M.S. thesis, Department of Applied Psychology, Clemson University, 2014. [Online]. Available: https://tigerprints.clemson.edu/all_theses/1848/

[8] M. E. St. Pierre, S. Banerjee, A. W. Hoover, and E. R. Muth, "The effects of 0.2 Hz varying latency with 20-100 ms varying amplitude on simulator Discomfort in a helmet mounted display," Displays, vol. 36, pp. 1–8, Jan. 2015.

[9] M. Ramshaw and S. Cutchin, "Reducing Motionsickness Resulting From Movement inside Virtual Reality Environments," in International Conference on Artificial Reality and Telexistence Eurographics Symposium on Virtual Environments, 2020.

[10] S. Palmisano, R. S. Allison, and J. Kim, "Cybersickness in Head-Mounted Displays Is Caused by Differences in the User's Virtual and Physical Head Pose," Front. Virtual Real., vol. 1, p. 587698, Nov. 2020.

[11] R. H. Y. So, "An investigation of the effects of lags on motion sickness with a head-coupled visual display," in United Kingdom Informal Group Meeting on Human Response to Vibration, 1994.

[12] D. J. Chen, B. Bao, Y. Zhao, and R. H. Y. So, "Visually induced motionsickness when viewing visual oscillations of different frequencies along the fore-and-aft axis: keeping velocity versus amplitude constant," Ergonomics, vol. 59, no. 4, pp. 582–590, Apr. 2016.

[13] R. H. Y. So, W. T. Lo, and A. T. K. Ho, "Effects of Navigation Speed on Motionsickness Caused by an Immersive Virtual Environment," Hum. Factors J. Hum. Factors Ergon. Soc., vol. 43, no. 3, pp. 452–461, Sep. 2001.

[14] C. C. T. Guo, D. J. Z. Chen, I. Y. Wei, R. H. Y. So, and R. T. F. Cheung, "Correlations between individual susceptibility to visually induced motion sickness and decaying time constant of after-nystagmus," Appl. Ergon., vol. 63, pp. 1–8, Sep. 2017.

[15] B. Keshavarz, A. E. Philipp-Muller, W. Hemmerich, B. E. Riecke, and J. L. Campos, "The effect of visual motion stimulus characteristics on vection and visually induced motion sickness," Displays, vol. 58, pp. 71–81, Jul. 2019.

[16] F. Bonato, A. Bubka, and S. Palmisano, "Combined pitch and roll and cybersickness in a virtual environment.," Aviat. Space. Environ. Med., vol. 80, no. 11, pp. 941–5, Nov. 2009.

[17] A. Kemeny, P. George, F. Merienne, F. Colombet, and F. Mérienne, "New VR Navigation Techniques to Reduce Cybersickness," 2017.

[18] A. S. Fernandes and S. K. Feiner, "Combating VR Discomfort through subtle dynamic field-of-view modification," 2016 IEEE

Symp. 3D User Interfaces, 3DUI 2016 - Proc., pp. 201–210, 2016.

[19] S. Zhang, A. Kurogi, and Y. Ono, "VR Discomfort in continuous exposure to live-action 180°video," in 26th IEEE Conference on Virtual Reality and 3D User Interfaces, VR 2019 - Proceedings, 2019, pp. 1269–1270.

[20] N. Padmanaban, T. Ruban, V. Sitzmann, A. M. Norcia, and G. Wetzstein, "Towards a Machine-Learning Approach for Discomfort Prediction in 360° Stereoscopic Videos," IEEE Trans. Vis. Comput. Graph., vol. 24, no. 4, pp. 1594–1603, Apr. 2018.

[21] W. Kim, S. Lee, and A. C. Bovik, "VR Discomfort Versus VR Presence: A Statistical Prediction Model," IEEE Trans. Image Process., vol. 30, pp. 559–571, 2021.

[22] R. H. Y. So, C. M. Finney, and R. S. Goonetilleke, "Motionsickness susceptibility and occurrence in Hong Kong Chinese," in Contemporary Ergonomics, Taylor & Francis, 1999.

[23] B. Keshavarz, B. E. Riecke, L. J. Hettinger, and J. L. Campos, "Vection and visually induced motionsickness: how are they related?," Front. Psychol., vol. 6, p. 472, 2015.

[24] C. M. Oman, "Are evolutionary hypotheses for motionsickness 'just-so' stories?," in Journal of Vestibular Research: Equilibrium and Orientation, 2012, vol. 22, no. 2–3, pp. 117–127.

[25] G. H. Crampton, Motion and Space Discomfort. 1990.

[26] A. de Castro, S. Barbero, S. Ortiz, and S. Marcos, "Accuracy of the reconstruction of the crystalline lens gradient index with optimization methods from Ray Tracing and Optical Coherence Tomography data," Opt. Express, vol. 19, no. 20, p. 19265, Sep. 2011.

[27] G. M. Stratton, "Vision without inversion of the retinal image," Psychol. Rev., vol. 4, no. 4, pp. 341–360, Jul. 1897.

[28] R. S. Kennedy, N. E. Lane, K. S. Berbaum, and M. G. Lilienthal, "Simulator Discomfort Questionnaire: An Enhanced Method for Quantifying Simulator Discomfort," Int. J. Aviat. Psychol., vol. 3, no. 3, pp. 203–220, Jul. 1993.

[29] F. H. McColgin, "Movement Thresholds in Peripheral Vision," J. Opt. Soc. Am., vol. 50, no. 8, p. 774, 1960.

[30] S. P. McKee and K. Nakayama, "The Detection of Motion in the Peripherl Visual Field," Vision Res., vol. 24, no. l, pp. 25–32, 1984.

[31] H. Strasburger, I. Rentschler, and M. Jüttner, "Peripheral vision and pattern recognition: A review," J. Vis., vol. 11, no. 5, pp. 1–130, 2011.

[32] J. D. Moss, J. Austin, J. Salley, J. Coats, K. Williams, and E. R. Muth, "The effects of display delay on simulator Discomfort," Displays, vol. 32, no. 4, pp. 159–168, Oct. 2011.

[33] Power Analysis for Two-group Independent sample t-test | R DATA ANALYSIS EXAMPLES," 2008. [Online]. Available: https://stats.idre.ucla.edu/r/dae/power-analysis-for-paired-sample-t-test/. [Accessed: 09-Nov-2021].

[34] R. Eisinga, M. Te Grotenhuis, and B. Pelzer, "The reliability of a two-item scale: Pearson, Cronbach, or Spearman-Brown?," Int. J. Public Health, vol. 58, no. 4, pp. 637–642, 2013.

[35] N. Stein, D. C. Niehorster, T. Watson, F. Steinicke, K. Rifai, S. Wahl, M. Lappe, "A Comparison of Eye Tracking Latencies Among Several Commercial Head-Mounted Displays," I-Perception., vol. 12, no. 1, pp. 1-16, 2021.

Chan, Tsz Tai

Tsz Tai Chan received a B.Eng. in Mechanical Engineering (2017) and M.Phil. in Industrial Engineering and Decision Analytics (2021) from the Hong Kong University of Science and Technology. He has experience on various data analytics projects in manufacturing and healthcare industry. He is now working as an optical engineer at the Facebook Reality Lab. His main interests are computational models for analyzing visual data, especially 3D computer vision methods and their applications.

Wang, Yixuan

Yixuan Wang received a BSc in Science (2017), majoring in Physics, from Liyun College, Beijing Normal University, Beijing, China. She is currently a PhD student at the Hong Kong University of Science and Technology, under the supervision of Prof. Richard So. Her research interests include investigating behavioral and physiological indicators, modeling individual differences in visually induced motion sickness and exploring the mechanism of visually induce motion sensations.

So, Richard Hau Yue

Prof. Richard SO received a B.S. in Electronics Engineering (1987) and Ph.D. in Applied Sciences (1995) from University of Southampton. He joined the Hong Kong University of Science and Technology in 1995 and is a Professor in Industrial Engineering and Decision Analytics. He studies human binocular vision and develops computational models of human vision. He is an elected Fellow of International Ergonomics Association, Chartered Institute of Ergonomics and Human Factors, and the Hong Kong Institute of Engineers. He has authored and co-authored more than 50 referred journal manuscripts and more than 100 conference papers.

Jia, Jerry

Jerry Jia is a system engineer and human perception specialist at Facebook Reality Lab. He advocates for user experience-centric product design and an integration of hardware system, algorithms and human vision system in product development for virtual reality and augmented reality applications. He received his Ph.D. in Material Science and Engineering from Columbia University in the City of New York (2011), B.S. in Physics (2005) and B.A. in Philosophy (2005) from Peking University in Beijing.